Synthesis and characterization of a polyaniline/HTiNbO$_5$ lamellar hybrid nanocomposite

Juanjuan Ma · Xiaobo Zhang · Chong Yan ·
Zhiwei Tong · Haruo Inoue

Abstract Polyaniline (PANI)/HTiNbO$_5$ lamellar hybrid nanocomposite was synthesized by the intercalation of aniline monomer into the layer structure of HTiNbO$_5$ followed by the subsequent in situ polymerization of aniline in the interlayer spacings. The synthesis process, the structure and morphology characterizations for lamellar hybrid nanocomposite were investigated by means of XRD, FTIR, TG–DTA, and SEM. Based on the experimental results, a detailed description of the conformation of polyaniline chains within the confined galleries of the inorganic host material was presented. TG analysis showed improved thermal stability for the intercalated nanocomposite in comparison with the pure PANI. Electrochemical studies indicated that the nanocomposite exhibited good redox activity and electrochemical-cycling stability.
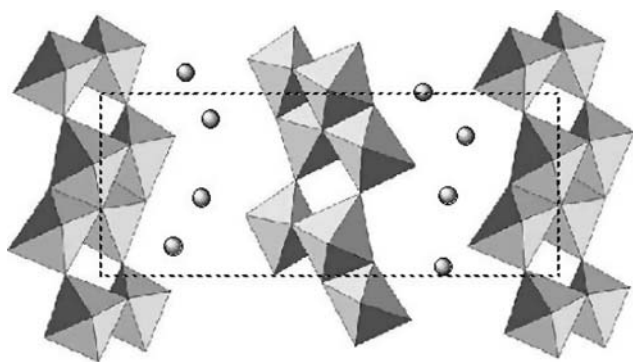
J. Ma (✉) · X. Zhang · C. Yan · Z. Tong
Department of Chemical Engineering, Huaihai Institute
of Technology, Lianyungang 222005, People's Republic
of China
e-mail: lanxuan98@gmail.com

J. Ma
Key Laboratory of Soft Chemistry and Functional Materials,
Ministry of Education, Nanjing University of Science and
Technology, Nanjing 210094, People's Republic of China

Z. Tong · H. Inoue
SORST, Japan Science and Technology (JST), Tokyo, Japan

H. Inoue
Department of Applied Chemistry, Graduate Course
of Engineering, Tokyo Metropolitan University,
1-1 Minami-ohsawa, Hachioji City, Tokyo 192-0397, Japan

Introduction

Layered compounds have been extensively investigated with purposes of producing advanced materials through the intercalation of guest species into the two-dimensional host interlayer region. Polymer intercalation nanocomposites prepared by using layered materials are expected to lead to a high degree of polymer ordering and exhibit advanced gas barrier, thermal stability, and enhanced mechanical properties compared to pristine polymers [1]. Polyaniline (PANI) is one of the most studied conducting materials due to its attractive properties such as high conductivity, simple synthesis, excellent environmental stability, as well as a large variety of applications especially in electronic devices [2], chemical sensors [3], separation membrane [4], etc. Recently, there are many published reports focusing on the preparation and new property studies of novel nanocomposites consisting of PANI with various layered materials, such as VOPO$_4$ · 2H$_2$O [5], MoO$_3$ [6], V$_2$O$_5$ [7, 8], FeOCl [9], and clay minerals [10–12]. However, a strong oxidizing layered compound is required to ensure polymerization as well as intercalation of aniline during the preparation of the hybrid. Some key problems related to mechanisms and properties are still ambiguous. Additionally, since such compounds are photochemically inactive, the application of these kinds of hybrid would be limited.

Among the many inorganic host materials, two-dimensional semiconducting crystallites of titanium oxide and niobium oxide have attracted great interest [13, 14]. Compared with other layered compounds, these nanosheets possess a high negative charge density, a high anisotropy, and an ultrathin thickness, which make them show distinctive conductivity and photo-response based on bandgap transitions [15, 16]. In present work, KTiNbO$_5$ was chosen as inorganic matrix due to its perfect lamellar structure and

Fig. 1 Structure of KTiNbO$_5$. Squares represent the TiO$_6$ (and NbO$_6$) octahedra and circles indicate the exchangeable cation K$^+$ in the interlayer

well-defined surface chemistry, contrary to layered silicate clays [17]. As shown in Fig. 1, KTiNbO$_5$ is a white solid in which the alkali ions lie between layers built up from zigzag chains of edge-sharing MO$_6$ octahedra [18]. H$^+$-exchanged form of KTiNbO$_5$ is relatively strong solid Brønsted acid and has no oxidizing ability. The intercalation of aniline into HTiNbO$_5$ can be carried out through acid–base neutralization followed by the polymerization initiated by an external effect. Consequently, the utilization of HTiNbO$_5$ as a host material is expected to favor the controllability of the polymerization process and expand the application of the hybrid.

Although some scientists have performed experiments for the layered titanoniobates as precursors to nanocomposites, there is not sufficient research for the morphology change of the interlayer structure. In this study, scanning electron microvoltage (SEM) permits direct observation of microstructural features formed during intercalation and polymerization. Based on the experimental results, we proposed the mechanism for the formation of PANI/layered host nanocomposite. In addition, the thermal degradation behavior of PANI chains in titanoniobate nanosheets prepared by in situ intercalative polymerization was first discussed through the thermogravimetric–differential thermal analysis (TG–DTA). Finally, we have also tested the electrochemical behavior of the nanocomposite.

Experimental

Materials

A layered compound KTiNbO$_5$ was synthesized by heating homogeneously mixed powders of K$_2$CO$_3$, TiO$_2$ and Nb$_2$O$_5$ (anatase, high-purity chemicals) in molar ratios of 1:2:1 at 1150 °C, according to the procedure described in the literature [19]. HCl and (NH$_4$)$_2$S$_2$O$_8$ were of AR grades. Aniline was distilled in vacuum prior to use.

Preparation of PANI/HTiNbO$_5$ nanocomposite

The protonated form HTiNbO$_5$ was obtained by the treatment of KTiNbO$_5$ with 6 M HCl for 24 h three times at room temperature. The intercalation of aniline into the interlayers of HTiNbO$_5$ was carried out as follows: 1 g HTiNbO$_5$ was dispersed in 20 mL distilled water and then 2 mL aniline was added dropwise to the suspension. The reaction mixture was maintained under vigorous stirring for 30 days at room temperature. The dispersion was centrifuged and washed with distilled water and methanol several times and then dried at 50 °C under vacuum overnight to obtain the white powder of ANI/HTiNbO$_5$ hybrid.

A 1 g sample of the ANI/HTiNbO$_5$ hybrid was added to an aqueous solution of a mixture of 10 mL (NH$_4$)$_2$S$_2$O$_8$ (1 M) and HCl (0.1 M), then stirred at 50 °C for 3 days. A color change from white through blue to dark was observed during the polymerization. The final nanocomposite (termed as PANI/HTiNbO$_5$) was centrifuged and washed with distilled water and dried at 50 °C in vacuum overnight.

Original PANI was prepared as follows: 5 mL aniline monomer was dissolved in 120 mL 1 M HCl. Then aqueous solution of (NH$_4$)$_2$S$_2$O$_8$ (12.3 g was dissolved in 50 mL water) was added dropwise to the above solution under stirring. The polymerization was allowed to proceed for 3 h at ca. 5 °C. The product was washed with distilled water and methanol several times and then dried at 50 °C under vacuum overnight.

Characterization

Scanning electron micrograph (SEM) images were taken with a JSM-5600 apparatus (JEOL) operating at 20 kV for the Au-coated samples. X-ray diffraction (XRD) patterns were obtained with a RINT 2000 diffractometer (Rigaku), using Cu Kα radiation ($\lambda = 0.154$ nm) with 2θ from 2.5° to 40°. Data were collected at a scanning rate of 1.0° min^{-1}. The infrared spectrum was recorded on a Shimadzu FTIR-8400S spectrometer with the use of KBr pellets. Thermal gravimetric analysis (TGA) was carried out with a Shimadzu DTG-60 apparatus under aerated conditions at a heating rate of 20 °C min^{-1}.

Electrochemical measurements were performed with a three-electrode electrochemical cell, with a platinum wire being used as the counter electrode, and a saturated calomel electrode as the reference electrode. The glassy carbon electrode (area 0.38 cm^2) was hand polished directly with a slurry of 1.0 and then 0.3 μm alumina (Buehler) and used as the working electrode. The PANI/HTiNbO$_5$ nanocomposite and original PANI films were deposited onto the glassy carbon electrode. Cyclic voltammetry (CV) scans

were carried out in 0.1 M HCl solution at a scan rate of 30–500 mV s^{-1} between −0.8 and 0.6 V.

Results and discussion

Synthesis of PANI/HTiNbO$_5$ hybrid compound

The intercalation of bulky ions into the interlayer spaces of titanoniobates is difficult owing to the high charge densities of $TiNbO_5^-$ layers. The protonation of KTiNbO$_5$ to give titanoniobic acid (HTiNbO$_5$) was carried out by the addition of HClaq (6 M) into the interlayers. Strong electrical attraction between the anilinium ions and the negative ($TiNbO_5^-$) layers is the driving force of the intercalation [17]. Figure 2 shows a sequence of SEM of KTiNbO$_5$ as starting material (a), after acid treatment (b), after intercalation in the presence of aniline (ANI/HTiNbO$_5$) (c), and after in situ polymerization (PANI/HTiNbO$_5$) (d). From Fig. 2a, we can see that the original KTiNbO$_5$ consists of plate-like texture reflecting its layered structure. The texture of the particles remains almost unchanged after the acid treatment process (Fig. 2b). However, with the intercalation of aniline, the exfoliation commences at the fringe of crystallite as shown in Fig. 2c. Interestingly, the resulting product PANI/HTiNbO$_5$ retains significantly the nanolayer structure from the starting crystallite, despite the fact that the overall crystallinity has decreased and most crystals appear multiply cleaved (Fig. 2d). This phenomenon may be explained by the rearrangement of monomer units during the polymerization.
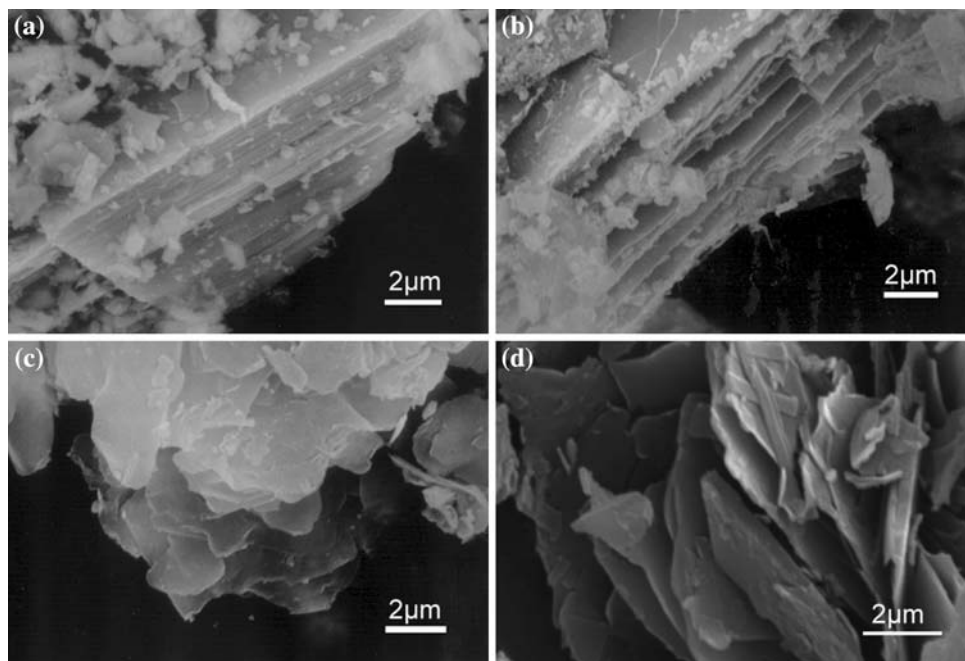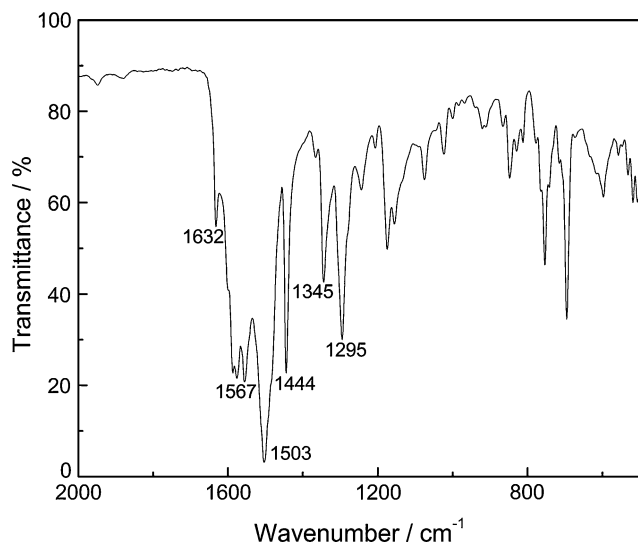
Figure 3 presents the XRD patterns of KTiNbO$_5$, HTiNbO$_5$, ANI/HTiNbO$_5$, and PANI/HTiNbO$_5$. The presence of a low-angle reflection at 10.51° 2θ ($d = 0.84$ nm) in the diffraction pattern of HTiNbO$_5$ indicates that the interlayer gallery is reduced by 0.08 nm relative to the starting material KTiNbO$_5$, which has a low-angle peak at 9.58° 2θ ($d = 0.92$ nm). Taking into account the diameter (ca. 0.24 nm) of the interlayered K$^+$ cation, we can get the thickness of $TiNbO_5^-$ slab (0.68 nm). By subtracting the thickness of $TiNbO_5^-$ slab, the net interlayer height of ANI/HTiNbO$_5$ and PANI/HTiNbO$_5$ is 0.62 and 0.50 nm, respectively. These expansions indicate that a monolayer of
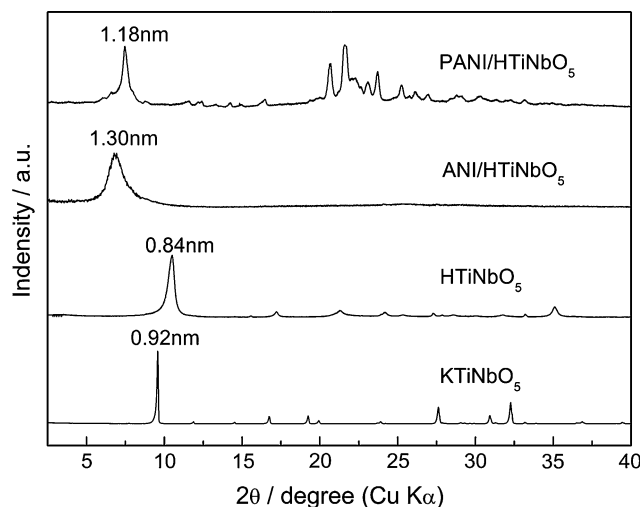
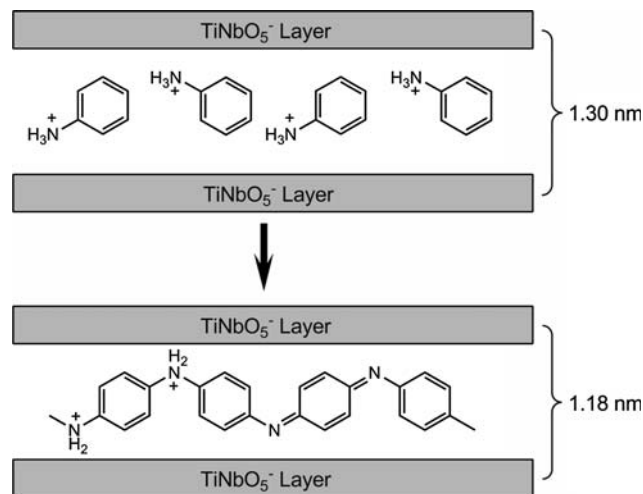**Fig. 3** XRD patterns of KTiNbO$_5$, HTiNbO$_5$, ANI/HTiNbO$_5$, and PANI/HTiNbO$_5$

Fig. 2 SEM micrographs of (**a**) KTiNbO$_5$, (**b**) HTiNbO$_5$, (**c**) ANI/HTiNbO$_5$, and (**d**) PANI/HTiNbO$_5$

Fig. 4 Infrared spectrum of PANI/HTiNbO$_5$ nanocomposite

Fig. 5 Proposed mechanism for the intercalation and polymerization of aniline between TiNbO$_5$$^-$ interlayers

monomers and a monolayer of polymers are formed and are comparable to the published value of ca. 0.70 nm in PANI/MoO$_3$ [6], 0.52 nm in PANI/V$_2$O$_5$ [8], and ca. 0.50 nm in PANI/FeOCl [9]. Moreover, the layer distance begins to shrink as the polymerization progressed, presumably due to the chemical bonding of the aniline monomers. It is worth noting that new diffraction peaks appear at around 18–22° in the XRD pattern of PANI/HTiNbO$_5$, which suggests the regularities in the arrangement of monomer unit during polymerization in the layer gallery [20]. This is in accordance with the SEM result for PANI/HTiNbO$_5$.

FT-IR spectroscopy also confirms that PANI has been successfully synthesized within the TiNbO$_5$$^-$ layers. In Fig. 4, a number of characteristic absorption bands of PANI can be observed at 1632 cm^{-1} (v(C=N)), 1567 cm^{-1} (quinoid ring v(C=C)), 1502 and 1444 cm^{-1} (benzenoid ring v(C=C)) [21]. The peaks at 1345 and 1295 cm^{-1} are associated with the C–N stretching mode. As reported by Louarn et al. [22], the existence of peaks in the vicinity of 1300–1350 cm^{-1} inherently corresponds to the protonation process via polysemiquinone radical formation mechanism, and none of the basic form gives rise to vibrational modes in this spectral region. Therefore it can be used as a direct proof to show if PANI is in its conducting state. It is possible to make a conclusion here about the coexistence of nonconducting form (emeraldine base) and conducting form (emeraldine salt) of PANI in the hybrid compound.

Based on the above experimental results, the proposed mechanism for the formation of PANI/layered host nanocomposite is shown in Fig. 5. When the polymerization occurs between the adjacent TiNbO$_5$$^-$ layers, the confined environment, where the slabs of inorganic host serve as a template, leads to form a relatively ordered polymer chain structure. This long-range order could be achieved by the

orientation of the polymer chains along certain crystallographic directions. According to XRD analysis, the height of PANI in TiNbO$_5$$^-$ layer is almost the same as those of other PANI-intercalated layered materials reported in the literature [8, 9]. This fact indicates that the benzene rings of PANI are arranged in zigzag conformation and the two-fold symmetry axis bisecting the C–N–C angle is perpendicular to the TiNbO$_5$$^-$ slabs. It should be noted that when PANI is inserted into the inorganic galleries the strong intermolecular interaction of PANI chains was eliminated by the host barriers and PANI single chain with an extended-chain conformation can be obtained, while it is impossible for normal polymerization of aniline. On the other hand, the polymerization is much slow in the confined environment. The time required for the reaction mixture to turn dark blue is more than 4 h. It is well known that generally aniline polymerization is a typical precipitation with a high reaction rate. In the case of intercalation polymerization, the limited interlayer space of the inorganic host material retards the diffusion of the radicals and the orientation of the aniline monomers and PANI oligomers.

Thermal analysis

Figure 6 shows the TG–DTA curves for a pristine KTiNbO$_5$ and a PANI/HTiNbO$_5$ nanocomposite. The thermal behavior of the PANI/HTiNbO$_5$ nanocomposite exhibits a three-step weight loss process. The first weight loss below 100 °C is caused by the vaporization of water. The second one in the temperature range from 100 to 500 °C is ascribed to the elimination of dopant (HCl). The third weight loss above 500 °C is believed to be due to the decomposition of PANI between the layers. In the DTA curve of PANI/HTiNbO$_5$ as shown in the inset figure, the
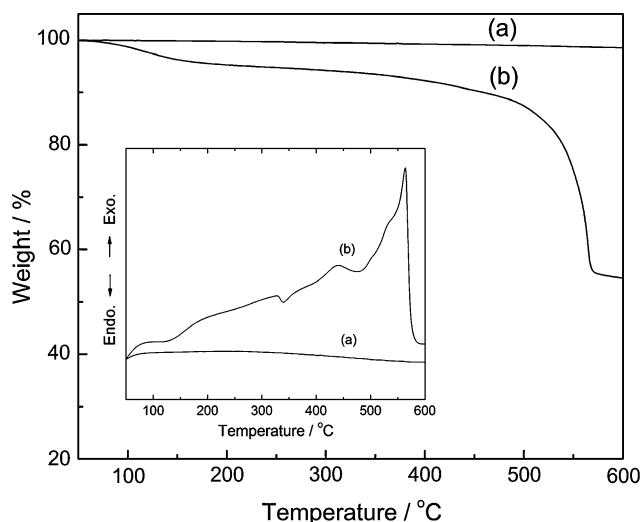
Fig. 6 TG–DTA curves (inset) of (a) pristine KTiNbO$_5$ and (b) PANI/HTiNbO$_5$ nanocomposite

exothermic peak ascribed to the decomposition of PANI appears at 564.1 °C, while the temperature for pure PANI is 530.6 °C [23]. This result suggests that the intercalated nanocomposite system is more thermally stable. It can be inferred that in the case of PANI/HTiNbO$_5$ the nanolayers act as barriers, blocking the degradation of PANI in the nanogalleries and also hindering the diffusion of degraded PANI from the nanocomposite.

Electrochemical studies

Figure 7 gives the CVs of a glassy carbon electrode modified with PANI/HTiNbO$_5$ nanocomposite measured at
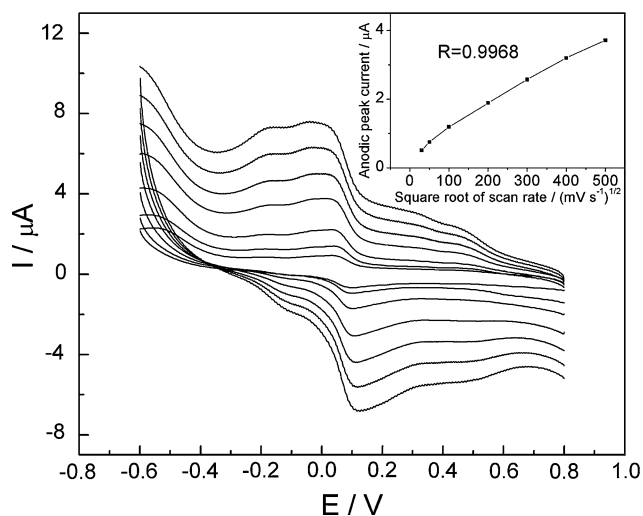
Fig. 7 Cyclic voltammograms of a glassy carbon electrode modified with PANI/HTiNbO$_5$ composite recorded in 0.1 M HCl at a scan rate of 30, 50, 100, 200, 300, 400, 500 mV s^{-1}, respectively. Inset shows the relationship between anodic peak current and scan rate

different scan rates. It is very clear that the PANI/HTiNbO$_5$ film exhibits very good redox activity in 0.1 M HCl. Two separate redox peaks (at −0.18 and −0.02 V) correspond to two redox processes of PANI normally found in acid conditions, i.e., transition between fully reduced leuco-emeraldine state (LM) and half-oxidized emeraldine state (EM), and transition between EM state and fully oxidized pernigraniline state (PE) [24]. The inset reveals that the anodic peak current is linearly proportional to the square root of scan rate, indicating a diffusion-controlled redox process. This electrochemical behavior of PANI/HTiNbO$_5$ nanocomposite is similar to that of PANI/polyelectrolyte system [25], but different from that of a modified Au nanoparticle prepared by LBL method [26, 27], which show a surface-controlled mechanism.

The stability of the obtained PANI/HTiNbO$_5$ nanocomposite is a key aspect for its practical application. Figure 8a shows the CV curves upon repeated potential
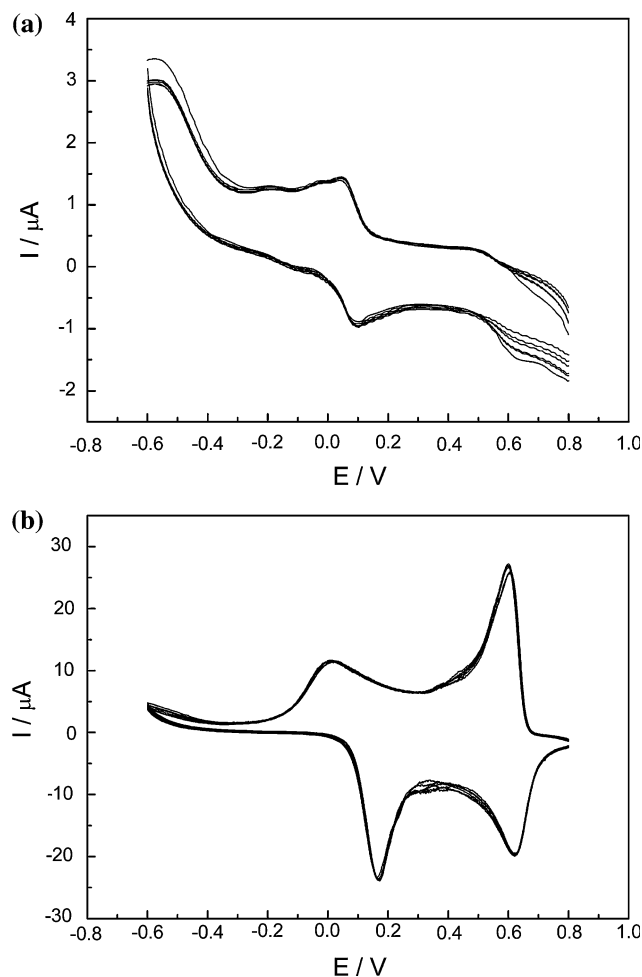
Fig. 8 Cyclic voltammograms upon repeated potential scans (−0.8 V ≤ E ≤ +0.6 V) of samples recorded in 0.1 M HCl at a scan rate of 50 mV s^{-1}: (a) PANI/HTiNbO$_5$ composite and (b) original PANI

cycling in the potential range between −0.8 and +0.6 V. The voltammograms of original PANI were also measured under the same condition (Fig. 8b). It can be seen that both PANI/HTiNbO$_5$ nanocomposite and original PANI are very stable in acid conditions, with almost no observable changes in both the peak current and the peak-to-peak separation after the first cycle. Thus, the excellent electrochemical stability and reproducibility of the nanocomposite are not affected by the presence of layered host material, which offer interesting opportunities for practical applications.

Conclusion

The intercalation of aniline into the layered titanoniobate semiconductor and the subsequent in situ polymerization of aniline were performed to develop an organic/inorganic hybrid material with interesting characteristics. Aniline monomers were successfully intercalated and polymerized within titanoniobate nanosheets in a monolayer structure, as confirmed by XRD, IR, and SEM. TG–DTA analysis indicated that the obtained polyaniline/HTiNbO$_5$ lamellar hybrid nanocomposite was more thermally stable than the pure PANI. In addition, the nanocomposite showed good redox activity and electrochemical-cycling stability.

References

1. Jia W, Segal E, Kornemandel D, Lamhot Y, Narkis M, Siegmann A (2002) Synth Met 128:115. doi:10.1016/S0379-6779(01)00672-5
2. Belanger D, Ren XM, Davey J, Uribe F, Gottesfeld S (2000) J Electrochem Soc 147:2923. doi:10.1149/1.1393626
3. Huang JX, Virji S, Weiller BH, Kaner RB (2003) J Am Chem Soc 125:314. doi:10.1021/ja028371y
4. Huang SC, Ball IJ, Kaner RB (1998) Macromolecules 31:5456. doi:10.1021/ma971418t
5. de Farias RF, Airoldi C (2003) Solid State Sci 5:611. doi:10.1016/S1293-2558(03)00046-3
6. Posudievsky OY, Biskulova SA, Pokhodenko VD (2002) J Mater Chem 12:1446. doi:10.1039/b107909c
7. Pang SP, Li GC, Zhang ZK (2005) Macromol Rapid Commun 26:1262. doi:10.1002/marc.200500235
8. Wu CG, DeGroot DC, Marcy HO, Schindler JL, Kannewurf CR, Liu YJ et al (1996) Chem Mater 8:1992. doi:10.1021/cm9600236
9. Wu CG, Degroot DC, Marcy HO, Schindler JL, Kannewurf CR, Bakas T et al (1995) J Am Chem Soc 117:9229. doi:10.1021/ja00141a015
10. Wu Q, Xue Z, Qi Z, Wang F (2000) Polymer (Guildf) 41:2029. doi:10.1016/S0032-3861(99)00356-0
11. Kim BH, Jung JH, Hong SH, Joo J, Epstein AJ, Mizoguchi K et al (2002) Macromolecules 35:1419. doi:10.1021/ma010497c
12. Lee D, Char K, Lee SW, Park YW (2003) J Mater Chem 13:2942. doi:10.1039/b303235c
13. Prasad GK, Takei T, Yonesaki Y, Kumada N, Kinomura N (2006) Mater Lett 60:3727. doi:10.1016/j.matlet.2006.03.097
14. Inui Y, Yui T, Itoh T, Higuchi K, Seki T, Takagi K (2007) J Phys Chem B 111:12162. doi:10.1021/jp0747048
15. Sasaki T, Ebina Y, Kitami Y, Watanabe M, Oikawa T (2001) J Phys Chem B 105:6116. doi:10.1021/jp010421i
16. Nakato T, Miyamoto N (2002) J Mater Chem 12:1245. doi:10.1039/b202000a
17. Du GH, Yu Y, Chen Q, Wang RH, Zhou W, Peng LM (2003) Chem Phys Lett 377:445. doi:10.1016/S0009-2614(03)01202-8
18. Tong ZW, Shichi T, Takagi K (2002) J Phys Chem B 106:13306. doi:10.1021/jp021162f
19. Tong ZW, Shichi T, Oshika K, Takagi K (2002) Chem Lett 31:876. doi:10.1246/cl.2002.876
20. Tsotcheva D, Tsanov T, Terlemezyan L, Vassilev S (2000) J Therm Anal Calorim 63:133. doi:10.1023/A:1010140504579
21. Yoshimoto S, Ohashi F, Kameyama T (2005) J Polym Sci Pt B Polym Phys 43:2705. doi:10.1002/polb.20561
22. Prasad PN, Mark JE, Ting JF (1995) Polymers and other advanced materials emerging technologies and business opportunities. Plenum Press, New York
23. Lee D, Char K (2002) Polym Degrad Stabil 75:555. doi:10.1016/S0141-3910(01)00259-2
24. Prasad KR, Munichandraiah N (2002) Synth Met 126:61. doi:10.1016/S0379-6779(01)00496-9
25. Tian SJ, Baba A, Liu JY, Wang ZH, Knoll W, Park MK et al (2003) Adv Funct Mater 13:473. doi:10.1002/adfm.200304320
26. Tian SJ, Liu JY, Zhu T, Knoll W (2004) Chem Mater 16:4103. doi:10.1021/cm049211j
27. Liu JY, Tian SJ, Knoll W (2005) Langmuir 21:5596. doi:10.1021/la0501233